

Kamlet–Taft Solvatochromic Parameters of the Sub- and Supercritical Fluorinated Ethane Solvents

Anthony F. Lagalante, Robert L. Hall, and Thomas J. Bruno*

National Institute of Standards and Technology, Physical and Chemical Properties Division, 325 Broadway, Boulder, Colorado 80303

Received: January 6, 1998; In Final Form: June 16, 1998

The Kamlet–Taft parameters describing the dipolarity-polarizability, π^* , and hydrogen bond acceptor ability, β , for ethane and six fluorinated ethane solvents in the sub- and supercritical region of the phase diagram were measured using solvatochromic probe molecules. The measured ultraviolet electronic transitions of the solvatochromic probes in a given solvent were fitted to third-order polynomials in solvent density for all isotherms investigated. The values of π^* and β were calculated for each of the solvents as a function of the solvent density. Trends in π^* values were related to the degree of fluorination about the ethane molecule, while the average β values for all solvents were negative and were interpreted as an inability on the solvents part to act as hydrogen bond acceptors.

Introduction

One of the most comprehensive and widely used solvent scales for the understanding and prediction of solvent behavior is that of Kamlet and Taft.^{1–4} The Kamlet–Taft solvent parameters are the hydrogen bond donation ability α , the hydrogen bond acceptor ability β , the dipolarity-polarizability π^* , and a correction term, δ , to the dipolarity-polarizability to account for variations in solvent polarizability within a given solvent class. The use of solvatochromic probes for the characterization of the molecular environment of compressed gases, both above and below the critical point, has been reported for several gases.^{5–12} These studies qualitatively reinforce the well-documented enhanced solvent strength about the critical point of the solvent; however, quantitative use of these solvent parameters to model equilibrium data in supercritical fluids is scarce. Quantitative prediction of solution equilibrium is possible using the Kamlet–Taft solvatochromic parameters through a linear solvation energy relationship (LSER). The general form of the LSER is

$$\log K = a + b(\pi^* + c\delta) + d\alpha + e\beta + \dots \quad (1)$$

where K represents the equilibrium property to be modeled. The magnitude and the sign of the coefficients (a , b , c , d , e , ...) of the LSER provide insight into the important factors governing the modeled equilibrium property.

With the production phaseout of chlorinated solvents, as mandated by the Montreal Protocol, interest in alternative solvent technology has grown significantly. In many industrial applications, supercritical fluids are being evaluated as replacements for chlorinated solvents, and the need for a systematic replacement approach is obvious and pressing. The potential solvating powers of fluorinated supercritical solvents are predicted to be superior to CO_2 in the high-density region from a solubility parameter approach.¹³ The LSER approach has thus far been used to predict solid–fluid enhancement factors for supercritical CO_2 systems¹⁴ and water– CO_2 partition coefficients.¹⁵

In addition to their environmental acceptance, the fluorinated analogues of the chlorinated solvents are attractive because they are gases at ambient conditions with useful critical temperatures and critical pressures (see Table 1).¹⁶ The tunable solvent strength of supercritical fluids and the ease of postextraction solute recovery are the primary advantages of supercritical fluids over conventional solvents in extraction processes. Five of the fluorinated ethanes in Table 1 possess a permanent dipole moment in contrast to the most commonly used supercritical fluid, CO_2 ($\mu_{\text{CO}_2} = 0$). A permanent solvent dipole moment leads to strong dipole–dipole or dipole–induced dipole attractive forces in solution, resulting in enhanced solubilities for polar compounds.

In this study, π^* and β were measured for a set of six fluorinated ethane solvents and ethane in the gas, supercritical, and liquid regions of the phase diagram. The fluorinated ethane solvents included hexafluoroethane (R116), pentafluoroethane (R125), 1,1,1,2-tetrafluoroethane (R134a), 1,1,1-trifluoroethane (R143a), 1,1-difluoroethane (R152a), and fluoroethane (R161). 4-Nitroanisole and 4-nitrophenol were used as solvatochromic probe molecules to calculate π^* and β values.

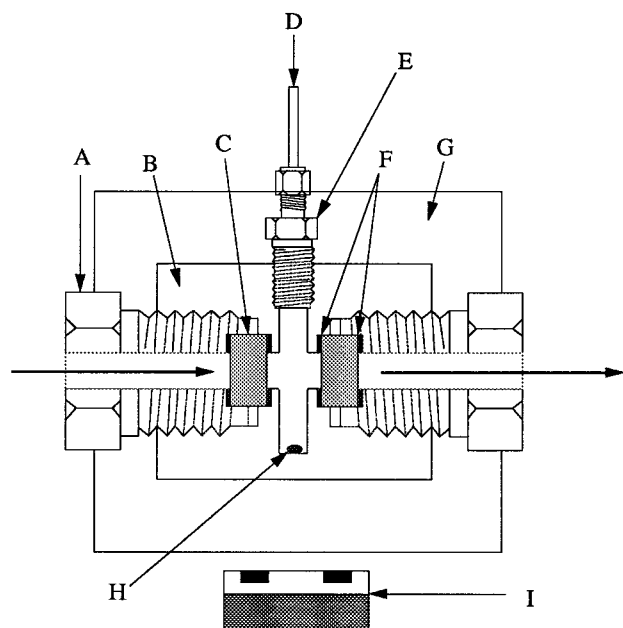
Experimental Section

Spectroscopic Cell Design. The high-pressure spectroscopic cell used for the measurement of the electronic transition maximum of the dissolved solvatochromic probes is depicted in Figure 1. The cell is machined from a cylinder (3.81 cm diameter, 5.08 cm length) of 316 stainless steel (AISI designation). At either end, a fitting with a 6.35 mm diameter bore was attached. Optical grade quartz windows (12.7 mm diameter, 6.35 mm thick) were recessed into the ends of each fitting, and a similar recess was machined into the interior of the cell body. The high-pressure glass-to-metal seal was accomplished using glass-filled polyether ether ketone (PEEK). A poly(tetrafluoroethylene)-coated magnetic stirring bar was placed in a 6.35 mm bore below the optical path. The stirring bar was coupled to NdFeB magnets mounted in a polyethylene disk and epoxied to a computer fan motor, as in previous cell designs.¹⁷ A pressure transducer, calibrated against a transfer standard

* To whom correspondence should be addressed. Fax 303-497-5224, e-mail bruno@boulder.nist.gov.

TABLE 1: Critical Properties and Dipole Moments of the Solvents Studied

solvent	T_c (°C)	p_c (MPa)	μ (D)
ethane	32.2	4.88	0
R116	19.9	3.04	0
R125	68.3	3.63	1.54
R134a	101.1	4.06	2.06
R143a	73.1	3.76	2.32
R152a	113.5	4.49	2.26
R161	102.2	4.70	1.94

**Figure 1.** Schematic of the high-pressure spectroscopic cell (arrows depict light beam path): (A) window fitting, (B) cell body, (C) quartz window, (D) solvent inlet line, (E) union fitting, (F) polyether ether ketone washers, (G) aluminum heating block, (H) magnetic stirring bar, (I) fan motor and NdFeB magnets

(traceable to a NIST dead weight pressure balance standard), was placed in line between the cell inlet and the outlet valve of the high-pressure syringe pump. The entire cell was thermostated inside of an aluminum heating block. Two 150 W cartridge heaters and a 100 Ω platinum resistance thermometer were embedded in the aluminum block. Temperature regulation (± 0.1 °C) of the heating block was provided by a microprocessor controller.

Chemicals. 4-Nitroanisole (99% purity) and 4-nitrophenol (99% purity) were obtained from a commercial supplier and were used as received. Ethane and the fluorinated ethane solvents (99.9+% purity verified by gas chromatography) were obtained from commercial suppliers and were used as received.

Measurement of Solution Spectra. A dual-beam, high-resolution, ultraviolet–visible spectrophotometer was used to determine the peak maximum of the electronic transition of 4-nitroanisole and 4-nitrophenol in each of the solvents. The aluminum heating block was preheated to the desired temperature and the spectroscopic cell placed inside and allowed to equilibrate at temperature. A small crystal of the solvatochromic probe was placed in the spectroscopic cell, and all transfer lines were connected. The valve to the cell was opened quickly, and the cell was flushed with gaseous solvent from the syringe pump. After the cell was then pressurized to a starting pressure of approximately 1.5 MPa, the stirring was continued until an equilibrium absorbance value of the probe molecule was obtained. The spectrum of the solvatochromic probe in the solvent was measured at a resolution of 0.05 nm per data point.

The electronic transition maximum of the dissolved solvatochromic probe was determined both by a peak detection algorithm of the spectrophotometer software package and by visual confirmation by the operator using an unsmoothed spectrum. The absorbance value at the transition maximum was maintained between 0.2 and 1.5 absorbance units at all times. A pressure reading was recorded from the inline pressure transducer, and a temperature reading was recorded from the digital controller. Pressure in the cell was changed incrementally with the syringe pump through the entire density range from gas (approximately 1.5 MPa) to liquid (20 MPa) states.

Calculation of the Kamlet–Taft Values. The π^* value¹ of the solvent was calculated using the measured frequency maximum (cm^{-1}) for the electronic transition of dissolved 4-nitroanisole ν_{NA} , using

$$\pi^* = (\nu_{\text{NA}} - 34170)/-2410 \quad (2)$$

The measured frequency maximum of 4-nitroanisole and 4-nitrophenol, ν_{NP} , was used to calculate β values² using

$$\beta = (-\nu_{\text{NP}} + 0.901\nu_{\text{NA}} + 4160)/2310 \quad (3)$$

Results

The measured frequencies (cm^{-1}) of both 4-nitroanisole and 4-nitrophenol were fit to a third-order polynomial of the form

$$\nu = A + B\rho + C\rho^2 + D\rho^3 \quad (4)$$

where the density ρ , expressed in mol L^{-1} , is the density of the pure solvent calculated using an extended corresponding states method with R134a as a reference fluid.¹⁸ Fitted constants to eq 4 for 4-nitroanisole and 4-nitrophenol, the correlation coefficient r , the standard deviation SD, and the total number of data points n for all isotherms measured are presented in Tables 2 and 3, respectively. The reported SD in each table is multiplied by a coverage factor,¹⁹ $k = 2$. The frequency values fitted to eq 4 correspond to densities spanning the gaseous state of the probe molecule ($\rho = 0$) to the solvent liquid-state density at 20 MPa. Although the frequency maxima of the two solvatochromic probes were measured on several isotherms for each fluorinated solvent, at constant density the frequency did not exhibit a temperature dependence. Measurement of 4-nitrophenol in R161 could not be performed due to the limited quantity of R161 available at the required purity.

To plot π^* and β as functions of the solvent density, the frequencies of the two solvatochromic probes were calculated from densities spanning the gas to liquid phase at density intervals of 0.5 mol L^{-1} using the constants in Tables 2 and 3. These calculated peak maxima values were used in eqs 2 and 3 to calculate π^* and β as a function of the solvent density. Figures 2 and 3 illustrate the density dependence of π^* and β , respectively.

Discussion

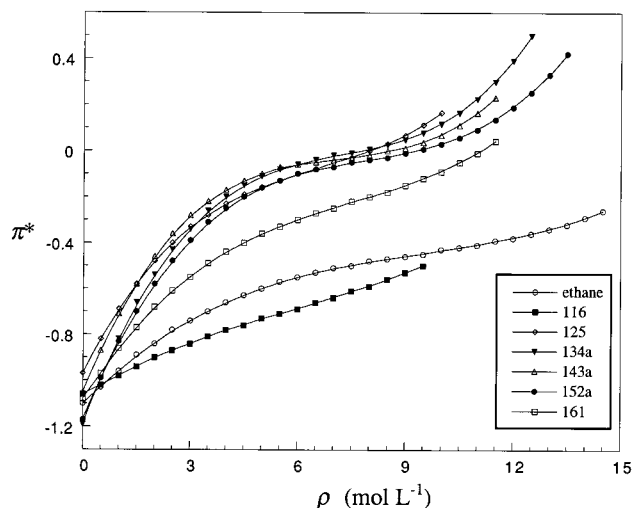
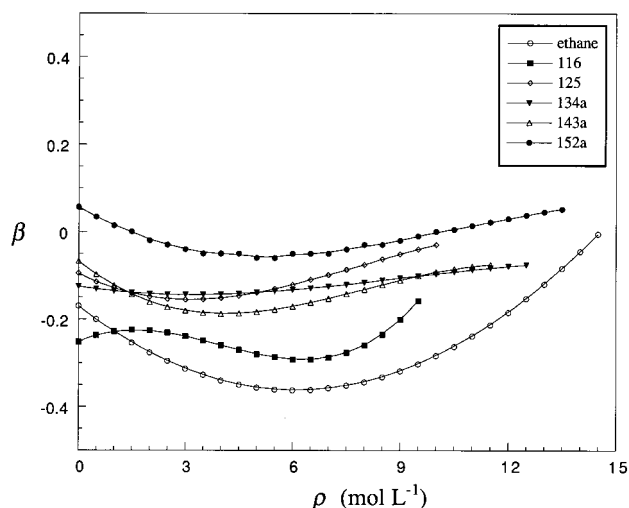
Work by Nicolet and Laurence has suggested that, rather than averaging several π^* values from different probes, 4-nitroanisole should be used as a standard for determining π^* values.²⁰ These authors have also reported on the temperature dependence of solvatochromism, or thermo-solvatochromism, and although in their work 4-nitrophenol and 4-nitroanisole did not exhibit a thermo-solvatochromism in the gas phase, in solution a thermo-solvatochromism was evident. In our study, we also found that increasing the solution temperature at constant pressure resulted in a shift in the frequency maximum to higher wavenumbers

TABLE 2: Fitted Constants to Eq 4 for 4-Nitroanisole in the Solvents Studied at the Given Temperatures

solvent	<i>T</i> (°C)	<i>A</i>	<i>B</i>	<i>C</i>	<i>D</i>	<i>r</i>	<i>k</i> SD	<i>n</i>
ethane	25, 35, 75, 100	36 826	−385.1	34.63	−1.220	0.996	0.100	56
R116	25, 50, 75, 100	36 740	−232.9	20.37	−1.143	0.988	0.094	55
R125	60, 80, 100, 110	36 510	−763.2	99.22	−5.029	0.982	0.200	35
R134a	50, 105, 120	37 040	−1028	131.9	−6.058	0.994	0.212	55
R143a	50, 75, 90	36 710	−941.2	124.8	−5.771	0.990	0.128	32
R152a	50, 80, 120, 140	36 980	−904.4	106.2	−4.462	0.993	0.232	56
R161	100, 120, 150	36 780	−596.8	64.18	−2.852	0.971	0.406	31

TABLE 3: Fitted Constants to Eq 4 for 4-Nitrophenol in the Solvents Studied at the Given Temperatures

solvent	<i>T</i> (°C)	<i>A</i>	<i>B</i>	<i>C</i>	<i>D</i>	<i>r</i>	<i>k</i> SD	<i>n</i>
ethane	25, 35, 75, 100	37 733	−199.3	18.77	−1.070	0.992	0.188	65
R116	25, 50, 75, 100	37 840	−298.1	53.35	−3.991	0.969	0.112	53
R125	60, 80, 100, 110	37 270	−588.9	69.50	−3.680	0.969	0.224	47
R134a	50, 105, 120	37 820	−895.6	113.0	−5.243	0.989	0.236	56
R143a	50, 75, 90	37 390	−692.8	86.90	−4.140	0.989	0.156	43
R152a	50, 80, 120, 140	37 350	−702.6	81.39	−3.570	0.986	0.196	48

Figure 2. Kamlet–Taft π^* values for the solvents studied.Figure 3. Kamlet–Taft β values for the solvents studied.

for both solvatochromic probes. The dependence on temperature is removed if the Kamlet–Taft values are plotted as functions of fluid density as in eq 4. A similar temperature independence has been previously reported for solvatochromic studies in supercritical fluids.¹¹

Other studies of solvatochromic probes in supercritical fluids have concentrated on measuring isotherms that are close to, and usually above, the critical temperature, concluding that the π^* values are separated into two linear regions that intersect at or

below the critical density of the solvent.^{5,11} The data from our measurements include data at subcritical temperatures and temperatures far above the critical point which support fitting the data to a third-order polynomial over the entire density range. The third-order polynomial gives a higher correlation coefficient with a lower overall standard deviation than fitting the data to two linear regions separated at the solvent critical point.

Our values of π^* for ethane in Figure 2 are in close agreement with the measured π^* values for ethane of Smith,⁵ who used 2-nitroanisole as a solvatochromic probe, and all curves project well to the gas-phase π^* value of -1.15 using 4-nitroanisole as the indicator.²¹ A trend in the degree of fluorination in the ethane backbone with π^* is readily discernible from the curves of Figure 2. As the degree of unsymmetrical fluorine substitution is increased from one to five fluorine atoms about the ethane backbone, a stepwise increase in the π^* curves is evident in Figure 2. Although R134a, R143a, R152a, and R161 have higher dipole moments than R125, the π^* values of R125 are similar in value to the others. The high number of electron-withdrawing fluorine groups in the molecule may cause the single proton in R125 to be extremely acidic, giving R125 a quasi-ionic nature and causing its π^* value to be unusually high. Indeed, R125 was found to be more reactive than the other fluorinated ethanes in this series when solubility measurements were made on a series of biomolecules.²² The π^* values of other fluorinated or perfluorinated alkanes are generally negative in value, as F and CF_3 are less polarizable than H and CH_3 .²³ This is in agreement with the fluorinated ethanes studied below the critical density of the solvent. At liquid densities, the π^* values of the fluorinated ethanes approach the values of their chlorinated analogues. For R143a, the π^* value at liquid densities is only slightly lower than that of 1,1,1-trichloroethane¹ ($\pi^* = 0.49$), suggesting that fluorinated solvents may be comparable to chlorinated solvents in strongly π^* -dependent LSER models. The π^* values for R161 are lower than the top four curves as is expected due to the lower dipole moment of R161. For ethane and R116, which possess no permanent dipole moment, the π^* values are low even when compared with a relatively nonpolar fluid such as hexane¹ ($\pi^* = -0.08$).

The commonly asserted notion of the “tunable solvent strength” for supercritical fluids is supported by the increasing π^* values of the curves in Figure 2. The solubility parameter of supercritical fluids is linearly related to the fluid density,²⁴ and consequentially the solvent strength is then directly proportional to the solvent density. This direct proportionality is not observed in the π^* values of Figure 2 possibly due to the fact that the solubility parameter concept is calculated from pure

fluid properties of the solvent, whereas the solvatochromic method is a direct measurement of a local solvent environment. The π^* curves do support the previously mentioned prediction that the fluorinated solvents will possess a greater solvent strength than CO_2 (π^* of liquid CO_2 is 0.04)⁵ based on a solubility parameter approach. The rate of change in π^* is greater for the more polar solvents, and the rate of change with density is not constant. In the low-density region, the solute–solvent interactions of the cybotactic region are only weakly interacting but increase rapidly as more solute molecules are added to the solution. At or slightly below the solvent critical density, a strong inflection occurs in the π^* curve, indicating that the solvation sphere is filled, and the rate of change in π^* decreases dramatically. Although the moles of solute are increasing in solution above the solvent critical density, the rate of change in the π^* curve is small possibly because the solvatochromic method only probes the immediate solute environment rather than the long-range interactions outside of the first solvation sphere. This immediate environment about the solute appears to remain relatively constant until the liquidlike density region, where the rate of change in π^* begins to increase again. Several plausible explanations of the π^* behavior in this high-density region are that either the solvatochromic probe may be influenced by solvent shells beyond the first solvation sphere, the increased pressure in this incompressible region increases the short-range attractive forces, or a solvent reorganization occurs to allow more solvent molecules to interact with the probe molecule.

The β values for the fluorinated solvents studied are shown in Figure 3. The measured values of β for the solvents are generally negative over the gas to liquid density range in the figure. The small oscillations in Figure 3 about an average value are within the experimental error of the measurements, and perhaps it is better to view β as an average value over the entire density range. Averaging β gives the following values ethane, -0.26 ± 0.10 ; R116, -0.25 ± 0.03 ; R125, -0.11 ± 0.04 ; R134a, -0.12 ± 0.02 ; R143a, -0.14 ± 0.04 ; and R152a, -0.01 ± 0.04 . It is expected that electronegative substituents will lower β values. For example, the β value for ethyl acetate is 0.45, while that for ethyl trichloroacetate is 0.25 and that for ethyl trifluoroacetate is 0.19.²⁵ Although negative basicity values are of no physical significance in the Kamlet–Taft solvent scale, it is nonetheless important to note that, in addition to the lack of a reproducible curve shape in Figure 3, there is no apparent trend in the solvent β values with fluorine substitution within experimental error. In comparison to reported results on the β value for supercritical CO_2 , our results are similar to the results of Sigman,⁷ who reported a constant value of β over all densities using 4-nitrophenol. We did not observe an increase in the β values with increasing density, as Ikushima¹⁰ observed for supercritical CO_2 using infrared stretching frequencies that are well correlated with the Kamlet–Taft β value.

The original β solvent scale of Kamlet and Taft was reevaluated by Laurence and Nicolet,^{20,26} who found a definite family dependence in β values for oxygen and nitrogen hydrogen bond acceptor solvents. They also found that the vibrational anomalies were minimal in the 4-nitrophenol and 4-nitroanisole pair as compared with other solvatochromic indicators and noted

that perfluorinated solvents were not included in the homomorphism line that defined the original solvatochromic equations. This last point may account for our measured negative β values of the fluorinated ethanes. The negative β values of both ethane and the fluorinated ethanes indicate that, within the parameters set forth by the original Kamlet–Taft β scale, these solvents are slightly poorer hydrogen bond acceptors in comparison to other solvents that are incapable of acting as acceptors a hydrogen bond. Since negative β values have been encountered in other studies of solvents above their critical points,⁷ it is a suggestion of the authors that the Kamlet–Taft β scale be reevaluated to include the effects of electron-withdrawing substituents, such as the fluorinated solvents studied herein, and a new zero point for the β scale established. In the future, we will report the use of the Kamlet–Taft values for the fluorinated solvents in a quantitative LSER approach to model supercritical fluid equilibrium.

Acknowledgment. A.F.L. acknowledges the financial support of the Professional Research Experience Program at the National Institute of Standards and Technology. Dana Defibaugh of NIST is acknowledged for providing R125.

References and Notes

- (1) Kamlet, M. J.; Abboud, J. L.; Taft, R. W. *J. Am. Chem. Soc.* **1977**, *99*, 6027.
- (2) Kamlet, M. J.; Taft, R. W. *J. Am. Chem. Soc.* **1976**, *98*, 377.
- (3) Kamlet, M. J.; Hall, T. N.; Boykin, J.; Taft, R. W. *J. Org. Chem.* **1979**, *44*, 2599.
- (4) Taft, R. W.; Kamlet, M. J. *J. Am. Chem. Soc.* **1976**, *98*, 2886.
- (5) Smith, R. D.; Frye, S. L.; Yonker, C. R.; Gale, R. W. *J. Phys. Chem.* **1987**, *91*, 3059.
- (6) Sun, Y.; Bennett, G.; Johnston, K. P.; Fox, M. A. *J. Phys. Chem.* **1992**, *96*, 10001.
- (7) Sigman, M. E.; Lindley, S. M.; Leffler, J. E. *J. Am. Chem. Soc.* **1985**, *107*, 1471.
- (8) Hyatt, J. A. *J. Org. Chem.* **1984**, *49*, 5097.
- (9) Kelley, S. P.; Lemert, R. M. *AIChE J.* **1996**, *42*, 2047.
- (10) Ikushima, Y.; Saito, N.; Arai, M.; Kunio, A. *Bull. Chem. Soc. Jpn.* **1991**, *64*, 2224.
- (11) Yonker, C. R.; Smith, R. D. *J. Phys. Chem.* **1988**, *92*, 235.
- (12) Yonker, C. R.; Frye, S. L.; Kalkwarf, D. R.; Smith, R. D. *J. Phys. Chem.* **1986**, *90*, 3022.
- (13) Roth, M. *Anal. Chem.* **1996**, *68*, 4474.
- (14) Bush, D.; Eckert, C. A. To be published in *ACS Symposium Series on Supercritical Fluid Extraction*; Abraham, M., Sunol, A., Eds.; American Chemical Society: Washington, DC, 1998.
- (15) Lagalante, A. F.; Bruno, T. J. *J. Phys. Chem. B* **1998**, *102*, 907.
- (16) Bruno, T. J. *Handbook for the Analysis and Identification of Alternative Refrigerants*; CRC Press: Boca Raton, FL, 1995.
- (17) Hansen, B. N.; Lagalante, A. F.; Sievers, R. E.; Bruno, T. J. *Rev. Sci. Instrum.* **1994**, *65*, 2112.
- (18) Huber, M. L.; Ely, J. F. *Int. J. Refrig.* **1994**, *17*, 18.
- (19) Taylor, B. N.; Kuyatt, C. E. *Guidelines for Evaluating and Expressing the Uncertainty of NIST Measurement Results*; National Institute of Standards and Technology: Washington, DC, 1994; Technol. Note 1297.
- (20) Nicolet, P.; Laurence, C. *J. Chem. Soc., Perkin Trans.* **1986**, 1071.
- (21) Essfar, M.; Guiheneuf, G.; Abboud, J. M. *J. Am. Chem. Soc.* **1982**, *104*, 6786.
- (22) Unpublished data.
- (23) Laurence, C.; Nicolet, P.; Dalati, M. T.; Abboud, J.-L. M.; Notario, R. *J. Phys. Chem.* **1994**, *98*, 5807.
- (24) Giddings, J. C.; Myers, M. N.; McLaren, L.; Keller, R. A. *Science* **1968**, *162*, 67.
- (25) Kamlet, M. J.; Abboud, J. L. M.; Abraham, M. H.; Taft, R. W. *J. Org. Chem.* **1983**, *48*, 2877.
- (26) Laurence, C.; Nicolet, P.; Helbert, M. *J. Chem. Soc., Perkin Trans. 2* **1986**, 1081.